Experimental and Numerical Sub-Interface Crack Paths

L. Marsavina[1], T. Sadowski[2], M. Knec[2]

[1] POLITEHNICA University of Timisoara, Timisoara, Romania, msvina@mec.upt.ro
[2] Lublin University of Technology, Lublin, Poland, t.sadowski@pollub.pl, m.knec@pollub.pl

ABSTRACT. *The presence of cracks has a major impact on the reliability of advanced materials, like fiber or particle reinforced ceramic composites, ceramic interfaces, laminated ceramics. For engineering application is very important to estimate the crack path, and the influence of the interface on the fracture parameters. This paper presents the particularities of sub-interface crack propagation near an interface with emphasizing crack path. The crack propagation algorithms for crack approaching interface and the implementation in the finite element analysis are shown. Experimental crack paths obtained during fatigue tests obtained using bi-material Four Point Bend Specimens are compared with the simulated ones.*

INTRODUCTION

The presence of cracks has a major impact on the reliability of advanced materials, like fiber or particle reinforced ceramic composites, ceramic interfaces, laminated ceramics. For engineering application is very important to estimate the crack path, and the influence of the interface on the fracture parameters.

The stress field around a crack paralleling an interface was introduced by Hutchinson et al. [1]. They connected the Stress Intensity Factors (SIF's) for crack paralleling the interface to the bi-material interface crack solution. A solution of stress intensity factors for bi-material Four Point Bend (FPB) specimens was provided by Marsavina and Piski [2], in analog manner with He and Hutchinson solution for homogeneous FPB specimen, [3].

A crack approaching an interface between two materials with different mechanical properties experiences changes in the stress field due to shielding or anti shielding effects and alter the stress intensity factor solutions, Marsavina and Sadowski [4]. Tilbrook et. al. [5], [6] used FPB specimens in order to investigate the influence of the interface on the crack tip parameters.

STRESS INTENSITY FACTORS SOLUTION FOR FOUR POINT BEND BI-MATERIAL SPECIMEN

Symmetric and asymmetric bi-material FPB specimens were adopted in experiments to investigate the influence of the interface on the crack path, Fig. 1. Bonding of the two

parts was done with Loctite Hysol 9461 epoxy based adhesive, after machining and cleaning of the surfaces (Loctite Cleaner 7061 and 7063). The notch was produced after the bonding by sawing with a razor-blade and diamond paste. Different values for the crack position *c* and crack length *a* were considered.

Solution of the homogeneous FPB was provided by He and Hutchinson [3]. In a similar way, Marsavina and Piski [2], proposed a solution of the bi-material FPB specimen loaded asymmetric. The loading configuration produces between the inner loading points a shear force *Q* and a bending moment *M* which could be expressed in the crack section:

$$Q = P\,(b_2 - b_1)/(b_2 + b_1)\,, \tag{1}$$

$$M = c\,Q \tag{2}$$

where b_1, b_2 and *c* are dimensions in [mm].

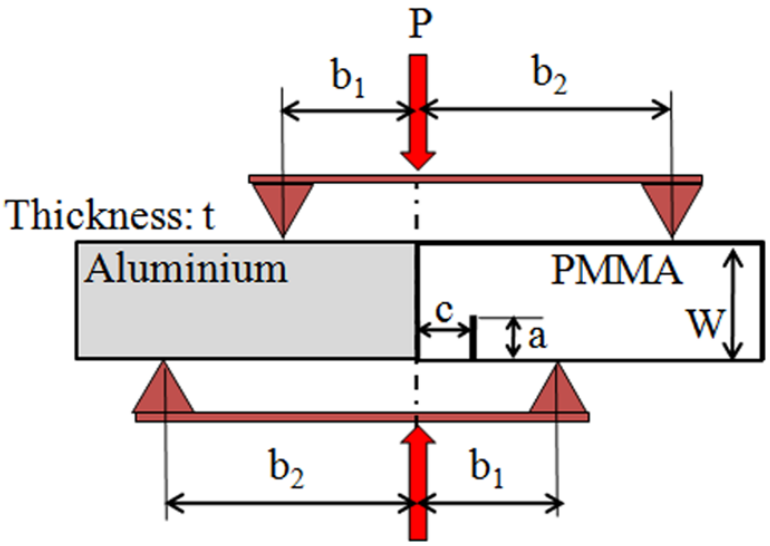

Figure 1. Geometry of the asymmetric bi-material FPB specimen.

Mode I Stress Intensity Factor (SIF) could be expressed in the following form, He and Hutchinson [3]:

$$K_I = \sigma\sqrt{\pi a}F_I\left(\frac{a}{W}\right), \tag{3}$$

where the crack opening is considered produced by bending moment *M*,

$\sigma = \dfrac{6(M - c_0 Q)}{W^2 t}$, *t*, *W*, *a* are specimen and crack dimensions, and

$$F_I\left(\frac{a}{W}\right) = 1.122 - 1.121\left(\frac{a}{W}\right) + 3.74\left(\frac{a}{W}\right)^2 + 3.873\left(\frac{a}{W}\right)^3 - 19.05\left(\frac{a}{W}\right)^4 + 22.55\left(\frac{a}{W}\right)^5 \quad \text{for } \frac{a}{W} < 0.7\,. \tag{4}$$

An additional term c_0 was introduced in order to take into account the finite width of the specimen, He and Hutchinson [3].

The mode II Stress Intensity Factor is expressed according to Murakami [7] in the form:

$$K_{II} = \eta\tau\sqrt{\pi a}\, F_{II}\left(\frac{a}{W}\right) \tag{5}$$

with $\tau = \dfrac{Q}{W \cdot t}$,

$$F_{II}\left(\frac{a}{W}\right) = -0.2915 + 6.3229\left(\frac{a}{W}\right) - 9.1199\left(\frac{a}{W}\right)^2 + 6.057\left(\frac{a}{W}\right)^3 \quad \text{for } 0.167 \le \frac{a}{W} \le 0.833, \tag{6}$$

and η a mode II correction factor, added to take into account the dimensions of specimen.

SIF's expressions (3) and (5) reduces to the solution corresponding to far loading points from crack for c_0=0 and η=1. A numerical solution of the bi-material FPB specimen made half of Aluminum and half of PMMA was provided by Marsavina and Piski [2]

Fig. 2.a presents the results of c_0/W for two ratios of c/W and for b_1/W=0.6. It could be observed that for small cracks and a zero bending moment in the crack position there is a significant K_I component for homogeneous material, while for bi-material specimen ratio c_0/W=0 for a/W>0.4, this means that SIF K_I decreases to zero. The mode II correction factor η versus a/W is plotted in Fig. 2.b for two crack positions. This correction factor has relevant values for short cracks being close to 1 for cracks with length a > 0.6 W in the case of homogeneous specimens, but is significantly lower than 1 for bi-material specimens.

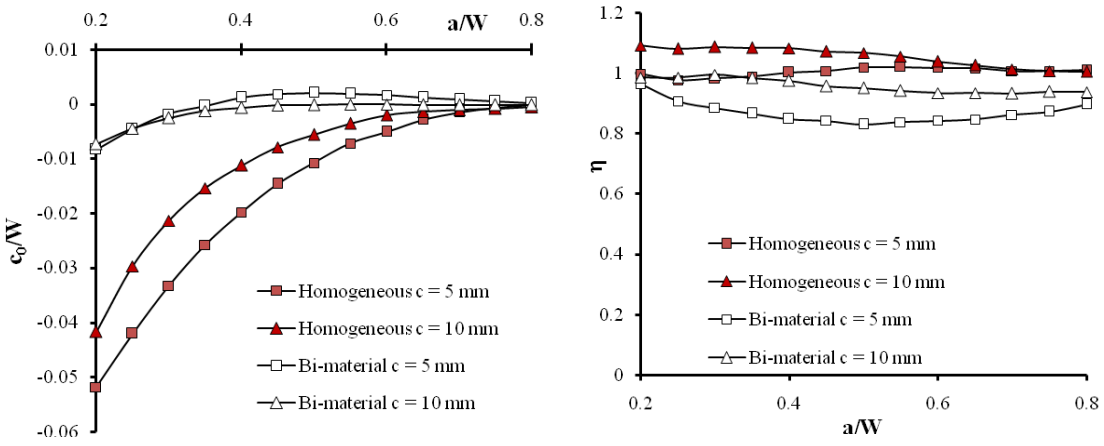

a. c_0/W mode I correction coefficient b. η mode II correction coefficient

Figure 2. Stress intensity factors correction coefficients for asymmetric FPB specimens

EXPERIMENTAL SET-UP

A MTS fatigue testing machine was used for fatigue bending tests, Fig. 3.a. Tests were performed at room temperature and with a frequency of 15 Hz. Different crack paths were obtained. To evaluate the crack path a digital camera was placed on one side of the specimen and after certain number of cycles images were recorded, Fig. 3.c. On the other side of the specimen an ARAMIS Digital Image Correlation system was used to track the crack path, Fig. 3.b.

a. Experimental set-up.

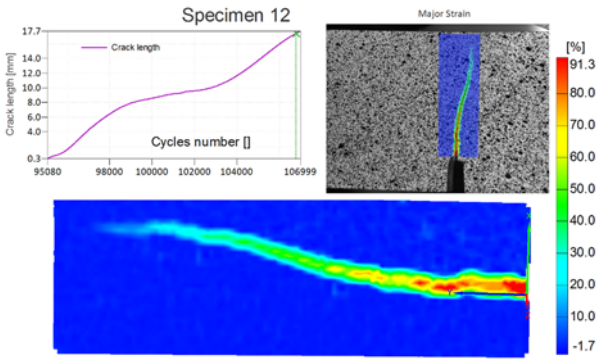

b. DIC identification of crack path

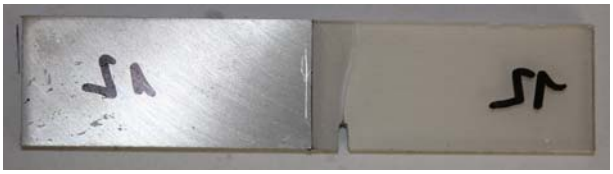

c. Digital camera image of crack path

Figure 3. Experimental set-up and crack path identification for specimen 12.

NUMERICAL SIMULATION OF CRACK PATH

Simulation of crack propagation was done using Finite Element Method implemented in FRANC2D/L code, developed at Cornell University, [8]. The numerical model was considered half of Aluminum (E_{Al} = 70 GPa, ν_{Al} = 0.33) and half of PMMA (E_{PMMA} = 3.25 GPa, ν_{PMMA} = 0.4), with dimensions used in the experiment, Fig. 1. Plane stress conditions with a thickness of 4 mm were considered. Different crack lengths and positions to the interface were considered. Eight node isoparametric elements were used to model the FPB specimen. Eight singular elements were placed around the crack tip as a common technique to model the stress singularity. A convergence study regarding the crack increment was performed on the specimen with a = 5 mm and c = 5 mm. After

this study a crack increment $\Delta a = a/10 = 0.5$ mm appears to give best results on reasonable computational time. The remesh and fill algorithm was used for the crack propagation studies [8]. Different crack propagation theories were considered maximum tensile stress [9], maximum energy release rate [10] and minimum strain energy density [11]. Finally, the minimum strain energy density method was adopted for the crack propagation studies. Fig. 4 presents the numerical model, a detail around the initial mesh and the obtained crack path for homogeneous and bi-material symmetric FPB specimen with $a = 5$ mm and $c = 5$ mm.

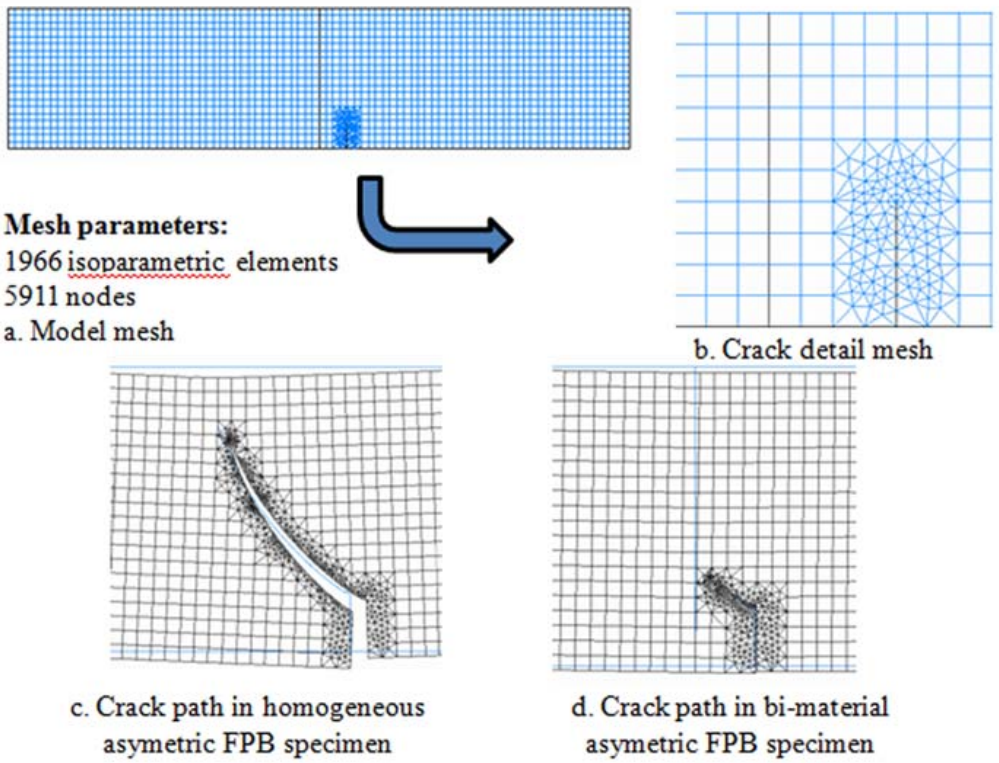

Figure 4. The mesh and deformed mesh for the asymmetric homogeneous and bi-material FPB specimens.

RESULTS AND DISCUSSIONS

Experimental and numerical crack path comparisons

Comparisons of experimental and numerical crack propagation paths for bi-material specimens are shown. Fig. 5.a presents the simulation and experimental results for experimental and numerical crack paths obtained for an initial crack with $a = 6.2$ mm and $c = 6.25$ mm loaded in predominantly mode I (symmetric loading with $F_{max} = 400$ N, $F_{min} = 100$ N and the interface in machine axis). It could be seen that the crack is pushed back by the interface. The crack paths are similar for the first 9 mm than the

experimental obtained crack path deviates, probably due to some movements of the specimens on the supports. For a predominantly mode II loading (asymmetric loading with F_{max} = 680 N, F_{min} = 295 N and the interface in machine axis) perfect matching between experimental and numerical crack paths were obtained, Fig. 5.b.

Curvilinear paths were obtained for crack propagation in both experimental and numerical investigations.

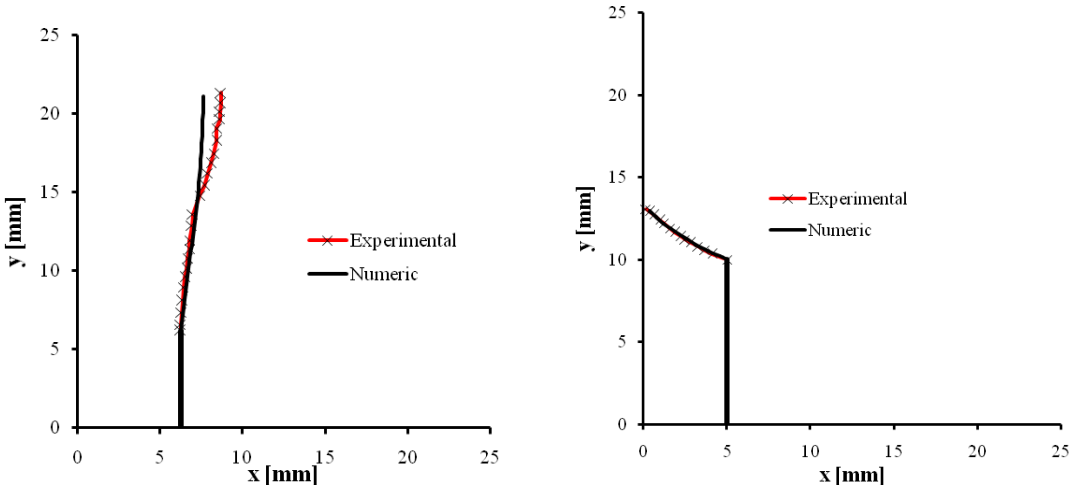

a. predominantly mode I loading b. predominantly mode II loading

Figure 5. Comparison between experimental and numerical crack paths for bi-material specimens in mixed mode loading.

Effect of material combination

In order to investigate the influence of material combinations on the crack path simulations were performed for symmetric and asymmetric FPB loadings considering three material combinations: homogeneous PMMA, Aluminium/PMMA and Aluminium/Al_2O_3 with the elastic properties shown in Table 1.

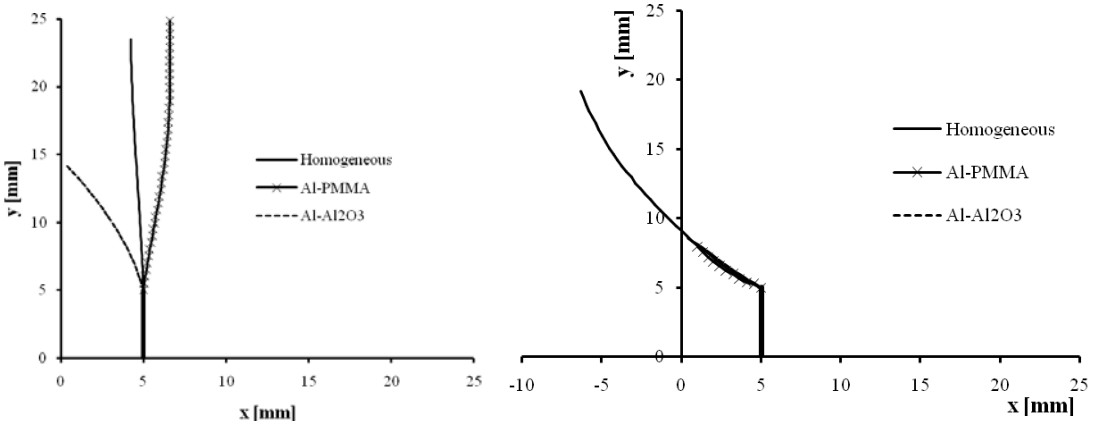

a. mode I loading b. mode II loading

Figure 6. Influence of material combination.

Fig. 6.a shows that the crack try to regain the symmetry for homogeneous specimen while different crack paths were obtained for bi-material specimens in mode I loading. When the crack is in the most compliant material (PMMA) the crack path looks to be pushed back by the interface. When the crack is in the stiffer material the crack propagate to interface.

For mode II loading the crack paths are similar for homogeneous and bi-material specimens up to interface.

Table 1. Mechanical properties

Material	Young Modulus E (MPa)	Poisson Ratio (-)
PMMA	3250	0.40
Aluminum	70000	0.33
Al_2O_3	400000	0.22

Effect of mode mixity

Different types of mode mixity were applied in the simulation starting from pure mode I for symmetric FPB specimen with the crack in the loading axis to pure mode II loading from asymmetric FPB specimen with the crack in the machine axis. The mode mixity is expressed by $\Psi = \text{atan}(K_{II}/K_I)$. However, due to the interface for pure mode II loading a mode I component is still present according to eq. (3). Fig. 7 shows that the applied mixed mode has an important effect on the resulting crack path.

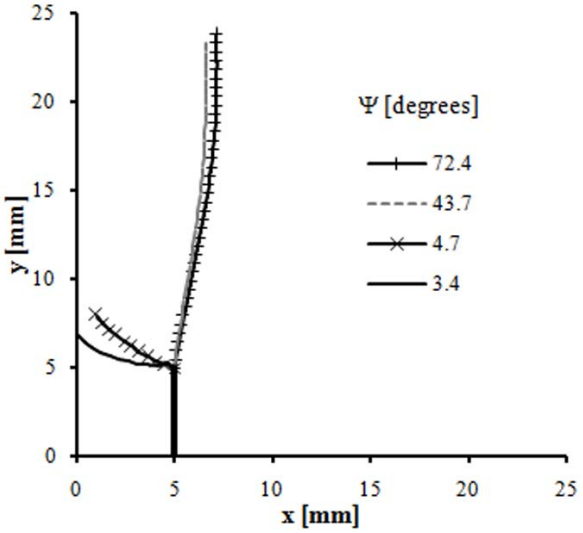

Figure 7. Influence of applied mixed mode

CONCLUSIONS

This work presents the experimental and numerical results of the influence of interface on the crack propagation path. Bi-material Four Point Bend specimens were used with symmetric and asymmetric loading. The following conclusions could be drawn:

- The presence of interface influences the crack propagation paths.
- Similar crack paths were obtained experimentally and numerically. The displacement correlation method for calculating the fracture parameters, the remesh and fill algorithm and the maximum principal stress criteria implemented in the Finite Element Analysis accurately predict the curvilinear crack propagation path.
- Crack propagation paths are influenced by the applied mixed mode load.
- The material combination has a significant role on the crack propagation path. When the crack is in the stiffer material will propagates toward the interface, and when is situated in the compliant material is push back by the interface.

ACKNOWLEDGMENTS

This research was supported by the FP7 European Reintegration Grant PERG03-GA-2008-230991, and the experimental work was done in the framework of the European Union Seventh Framework Programme (FP7/2007 – 2013), FP7 - REGPOT – 2009 – 1, under grant agreement No: 245479

REFERENCES

1. Hutchinson, J.W., Mear, M.E., Rice, J.R. (1987) *J. Appl. Mech.* **54**, 828-832.
2. Marsavina, L., Piski, T. (2010) *Int. J. Fracture* **164**, 325-332.
3. He, M.Y., Hutchinson, J.W. (2000) *J. Appl. Mech.* **67**, 207-209.
4. Marsavina, L., Sadowski, T. (2009) *Comp. Mater. Sci.* **45**, 693-697.
5. Tilbrook, M.T., Moon, R.J., Hoffman M. (2005) *Eng. Fract. Mech.* **72**, 2444–2467.
6. Tilbrook, M.T., Rozenburg, K., Steffler, E.D., Rutgers, L., Hoffman M. (2006) *Compos. Part B* **37**, 490–498.
7. Murakami, Y. (1987) *Stress Intensity Factors Handbook*, Pergamon Press, New York.
8. Wawrzynek, P.A., Ingraffea A.R. (1991) *Discrete modeling of crack propagation: theoretical aspects and implementation issues in two and three dimensions*, Cornell University, Ithaca.
9. Erdogan F., Sih G.C. (1963) *J. Basic Eng.* **85**, 519-525.
10. M. A. Hussain M.A., Pu, S.U., Underwood J. (1974) ASTM STP 560, 2-28.
11. Sih G.C. (1974) *Int. J. Fracture Mech.* **10**, 305-321.